


Article

Dynamic Shannon Performance in a Multiobjective Particle Swarm Optimization

E. J. Solteiro Pires ¹, J. A. Tenreiro Machado ^{2,*} and P. B. de Moura Oliveira ¹

¹ INESC TEC—INESC Technology and Science (UTAD pole), ECT—UTAD Escola de Ciências e Tecnologia, Universidade de Trás-os-Montes e Alto Douro, 5000-811 Vila Real, Portugal

² Department of Electrical Engineering, ISEP—Institute of Engineering, Polytechnic of Porto, Rua Dr. António Bernadino de Almeida, 4249-015 Porto, Portugal

* Correspondence: jtm@isep.ipp.pt

Received: 29 July 2019; Accepted: 20 August 2019; Published: 23 August 2019



Abstract: Particle swarm optimization (PSO) is a search algorithm inspired by the collective behavior of flocking birds and fishes. This algorithm is widely adopted for solving optimization problems involving one objective. The evaluation of the PSO progress is usually measured by the fitness of the best particle and the average fitness of the particles. When several objectives are considered, the PSO may incorporate distinct strategies to preserve nondominated solutions along the iterations. The performance of the multiobjective PSO (MOPSO) is usually evaluated by considering the resulting swarm at the end of the algorithm. In this paper, two indices based on the Shannon entropy are presented, to study the swarm dynamic evolution during the MOPSO execution. The results show that both indices are useful for analyzing the diversity and convergence of multiobjective algorithms.

Keywords: multiobjective particle swarm optimization; Shannon entropy; solution diversity; front level heterogeneity

1. Introduction

Multiobjective optimization (MOO) consists either in minimizing or in maximizing a set of objective functions subject to some constraints. In these problems, the objective functions are conflicting, leading to several vectors of decision variables. Each vector represents a possible solution that solves the problem with different trade-offs among the design objectives. Evolutionary and social-based algorithms have attracted the attention of many researchers, because they are frequently superior to conventional mathematical techniques due to their stochastic properties [1].

The MOO is inspired by biological phenomena and adopts a population that evolves during several generations. The PSO nature metaphor mimics the behavior of birds flocking or fish schooling [2]. Each bird or fish is represented by a particle with two components, namely by its position and velocity. A set of particles forms the swarm that evolves during several iterations giving rise to a powerful optimization method.

The particle swarm optimization's (PSO) simplicity and success led to its application in problems where more than one optimization criterion is considered. Many techniques, such as those borrowed from genetic algorithms (GA) [3,4], have been developed to find a set of solutions belonging to the Pareto front. Since the multiobjective PSO (MOPSO) proposal [5], the algorithm was used in a wide range of applications [6,7], and a considerable number of variants of refined MOPSO were developed in order to improve its performance [8,9].

The performance of multiobjective algorithms is usually analyzed at the end of their execution, and its success is measured by means of several metrics proposed in the literature [10]. Additionally, in ambiguous situations, the use of nonparametric tests can be adopted [11,12]. Some of the proposed

indices are based on Shannon entropy. Wang et al. [13] presented a method revealing interesting results: (i) the computational effort increases linearly with the number of solutions, (ii) the metric qualifies the combination of uniformity and coverage of the Pareto set, and (iii) it determines when the evolution has reached its maturity. LinLin and Yunfang [14] proposed a technique to measure the performance of multiobjective problems that not only indicates when the algorithm should be stopped, but can also compare the performance of multiobjective algorithms. The technique adopts entropy that is evaluated regarding the solution density in a gridded space.

Other studies tried to unravel the population dynamics during time evolution [15–20]. Farhang-Mehr and Azarm [15] developed an entropy-based metric to assess the diversity in a MOEA during the run time. To measure the entropy, a grid of cells was used, where solutions belonging to the same cell are considered identical. They orthogonalize and project them into a plane to count 3D nondominated solutions. Deb and Jain [16] proposed two multiobjective running metrics, one for measuring the convergence and the other for assessing the diversity among solutions. Myers and Hancock [17] suggested the use of the Shannon entropy to evaluate the run-time performance of a GA to solve labeling problems. The entropy measured in the parameter space is used to provide useful information about the algorithm state. Myers and Hancock concluded that populations with entropy smaller than a given threshold become saturated and their diversity disappears. Pires et al. [18] studied the signal propagation during the evolution of a GA. The mutation operator signal suffers a perturbation during some generations, and the corresponding fitness variation is analyzed. Pires et al. adopted the Shannon entropy to study the dynamics of MOPSO [19] and nonsorting GA II [20] during their execution. Wu et al. proposed a MOEA considering individual density (cell density) where the Shannon entropy was used to estimate the evolution state [21].

Taking these ideas in consideration, this paper studies the dynamics and self-organization of solutions during the MOPSO execution. The study analyzed two entropy indices considering three optimization functions with different swarm and archive sizes.

The main contributions of the paper are:

- New diversity indices inspired by physics and biologic systems.
- A good agreement of measures between the indices.
- Identification of stagnating states during the evolution.

Section 2 describes the method adopted in the work and includes a brief description of the main entropy concepts. Section 3 presents the indices for measuring the population diversity. Section 4 formulates the functions to be optimized and analyzes the simulations results. Finally, Section 5 outlines the main conclusions and the perspectives toward future work.

2. Methodology and Entropy Concepts

A careful look into MOPSO reveals a need to understand the dynamics during successive iterations with a particular focus on the particles' convergence to the nondominated front and particle diversity. For this purpose, the Shannon entropy is used in the follow-up, and a set of tests is performed considering different optimization functions and archive sizes. Since the MOPSO algorithm is stochastic, a battery of tests is required to generate a representative statistical sample [22].

The entropy is associated with several concepts and interpretations [23]. Boltzmann used entropy to describe systems that evolve from ordered to disordered states. *Spreading* was used by Guggenheim to indicate the diffusion of an energy system from a small to a large volume. Lewis stated that in a spontaneous expansion gas in an isolated system, *information* regarding the particles' locations decreases, while the missing information or *uncertainty* increases.

Shannon [24] developed a theory to quantify the information loss in the transmission of a given message. The study was carried out in a communication channel and focused on the physical and statistical constraints that limit the message transmission. Shannon defined entropy H as a measure of information, given by:

$$H(X) = -K \sum_{x \in X} p_i(x) \log p_i(x). \quad (1)$$

This expression considers a discrete random variable $x \in X$ characterized by the probability distribution $p(x)$. The parameter K is a positive constant, often set to 1, and is used to express H in a given unit of measure.

The Shannon entropy can be easily extended to multidimensional random variables. For a pair of random variables $(x, y) \in (X, Y)$, entropy is defined as:

$$H(X, Y) = -K \sum_{x \in X} \sum_{y \in Y} p_i(x, y) \log p_i(x, y). \quad (2)$$

3. Entropy Indices for Assessing the MOPSO

In this section, two indices for measuring the entropy in a MOPSO are presented. The first one captures the particle diversity, while the second addresses the front diversity.

3.1. Particle Diversity

The index to measure the particle diversity was proposed previously [25]. The index follows a particular interpretation of entropy. Indeed, entropy can express the spreading of a system energy from a 'better located' state to a 'more distributed' one. Taking this idea in mind, the minimum spanning tree that connects all the archive particles, A , where each connection belongs to the set of edges that connects all the $\#A$ particles with the minimal edge distance, was considered. Let d_i be one of these edges, where $i \in \{1, 2, \dots, \#A - 1\}$, and p_i is a probability given by the following Equation:

$$p_i = \frac{d_i}{\sum_{j=1}^{\#A-1} d_j}. \quad (3)$$

The particle diversity index is based on this point of view and can be represented as:

$$H(X) = - \sum_{i=1}^{\#A-1} p_i \log p_i. \quad (4)$$

3.2. Front Level Heterogeneity

In ecology, the diversity measure of different populations species is equated with the uncertainty that occurs when selecting randomly one individual species from the populations [26]. The information content, or population diversity, can be defined in several ways [27], and one of them is explained in the follow-up.

Consider a population with s species in proportion to $p_i = \frac{n_i}{\#A}$, i.e., $\{p_1, p_2, \dots, p_s\}$, where n_i is the number of elements of the i th species and s denotes the total number of species. Then the population diversity is given by Shannon and Weaver's formula [28]:

$$H'(X) = - \sum_{i=1}^s p_i \log p_i. \quad (5)$$

Taking this idea in mind, Expression (5) is used to measure the Shannon front level diversity, where n_i and s are the number of particles in each front and the total number of fronts, respectively. This index is called front level heterogeneity in order to avoid confusion with the particle diversity index. In MOPSO, at later evolution stages, when only the nondominated front exists in the swarm, the entropy heterogeneity $H'(X)$ is zero.

4. Simulations Results

This section presents the results obtained for 3 optimization problems $P_i, i = 1, 2, 3$, and different archive sizes. The dynamic behavior of algorithms was studied using the two proposed indices.

The optimization problems P_1 and P_2 (known as DTLZ2 and DTLZ4 [29]) are defined by Equations (6) and (7), and problem P_3 (known as UF8 in CEC 2009 special session competition [30]) is formulated in Equation (8) as follows:

$$\left\{ \begin{array}{l} \min P_1 = [f_{11}(X), f_{12}(X), f_{13}(X)] \\ f_{11}(X) = [1 + g_1(X)] \cos(x_1 \pi / 2) \cos(x_2 \pi / 2) \\ f_{12}(X) = [1 + g_1(X)] \cos(x_1 \pi / 2) \sin(x_2 \pi / 2) \\ f_{13}(X) = [1 + g_1(X)] \sin(x_1 \pi / 2) \\ g_1(X) = 1 + 9 \sum_{i=3}^m (x_i - 0.5)^2 \end{array} \right. \quad (6)$$

$$\left\{ \begin{array}{l} \min P_2 = [f_{21}(X), f_{22}(X), f_{23}(X)] \\ f_{21}(X) = [1 + g_2(X)] \cos(x_1^\alpha \pi / 2) \cos(x_2^\alpha \pi / 2) \\ f_{22}(X) = [1 + g_2(X)] \cos(x_1^\alpha \pi / 2) \sin(x_2^\alpha \pi / 2) \\ f_{23}(X) = [1 + g_2(X)] \sin(x_1^\alpha \pi / 2) \\ g_2(X) = 1 + 9 \sum_{i=3}^m (x_i^\alpha - 0.5)^2 \end{array} \right. \quad (7)$$

$$\left\{ \begin{array}{l} \min P_3 = [f_{31}(X), f_{32}(X), f_{33}(X)] \\ f_{31}(X) = \cos(0.5x_1\pi) \cos(0.5x_2\pi) + \frac{2}{|J_1|} \sum_{j \in J_1} g_j(X) \\ f_{32}(X) = \cos(0.5x_1\pi) \sin(0.5x_2\pi) + \frac{2}{|J_2|} \sum_{j \in J_2} g_j(X) \\ f_{33}(X) = \sin(0.5x_1\pi) + \frac{2}{|J_3|} \sum_{j \in J_3} g_j(X) \\ g_j(X) = \left(x_j - 2x_2 \sin(2\pi x_1 + \frac{j\pi}{m}) \right)^2 \\ J_1 = \{j | 3 \leq j \leq m, \text{ and } j + 2 \text{ is multiple of } 3\} \\ J_2 = \{j | 3 \leq j \leq m, \text{ and } j + 1 \text{ is multiple of } 3\} \\ J_3 = \{j | 3 \leq j \leq m, \text{ and } j \text{ is multiple of } 3\} \end{array} \right. \quad (8)$$

where m is the number of parameters, f_{ij} is the objective $j \in \{1, 2, 3\}$ of problem $i \in \{1, 2, 3\}$, and g represent some auxiliary functions in order to simplify the expressions. For $\{P_1, P_2\}$, the parameter intervals are set to $x_i \in [0, 1]$. In Equation (7), the parameter value $\alpha = 100$ allows a meta-variable mapping, $x_i \rightarrow x_i^\alpha$, between the two functions [29]. For $\{P_3\}$, $x_i \in [0, 1]$ if $i \leq 2$ and $x_i \in [-2, 2]$ if $2 < i \leq m - 2$. For $\{P_1, P_2, P_3\}$, the number of parameters is set to $m = \{12, 12, 30\}$.

These problems are to be optimized using a MOPSO [5,6], where the search is driven by a population of particles that move using the equations:

$$v_i^{t+1} = w \cdot v_i^t + \phi_1 \cdot \text{rand}(0, 1) \cdot (b_i - x_i^t) + \phi_2 \cdot \text{rand}(0, 1) \cdot (g_i - x_i^t), \quad (9)$$

$$x_i^{t+1} = x_i^t + v_i^{t+1}, \quad (10)$$

where t is the iteration number, w denotes the inertia coefficient, and the positions x_i and velocities v_i are codified by means of real numbers. In order to start with an high exploration rate of the search space, w is initialized with the value 0.7 and decreases linearly with t to 0.25. In the stages where w is near the value 0.25, more importance is given to the local search rather than the global one. In the particle motion, the same influence is given to the local best particle position b_i and the position of the 'best' particle g_i . Therefore, the cognitive and social coefficients are set to the values $\phi_1 = \phi_2 = 0.8$. In a nondominated set, there is no best solution. Consequently, to choose a particle with similar

characteristics while incorporating uncertainty, a particle determines its ‘global best’, or guide, by randomly selecting three particles from the archive and picking up the nearest particle g_i .

The archive is updated, at the end of each iteration, using a $(\mu + \lambda)$ strategy among the archive, $\#\mu$, and swarm, $\#\lambda$, solutions. Therefore, the best μ solutions are chosen among the archive and population solutions. The solutions are selected according to the maximin sorting scheme [12].

Four swarm sizes with $\#N = \{250, 300, 350, 400\}$ particles and four archive sizes of $\#A = \{50, 100, 150, 200\}$ particles are adopted, resulting in a total of 4^2 different experiments. For each experiment, 21 distinct runs were performed, their entropies evaluated, and the medians of the particles and the populations’ diversities and heterogeneities $H_m = \text{median}(H)$ and $H'_m = \text{median}(H')$ at each iteration t taken as representing the entropy evolution at that instant.

This section presents the entropy evolution for those experiments addressing the problems $\{P_1, P_2, P_3\}$.

4.1. Results of DTLZ Problems Optimization

The first optimization functions to be considered belong to problem P_1 , with three objectives described by Equation (6). Expressions (4) and (5) are adopted to monitoring the MOPSO evolution. The results are depicted in Figures 1 and 2 for archive sizes of $\#A_1 = 50$ and $\#A_4 = 200$ particles, respectively. The charts show the median entropies H_m and H'_m versus the iteration t , for experiments with $\#N = \{250, 300, 350, 400\}$ particles. The curves with the ‘solid’ and ‘dotted’ lines represent H_m and H'_m , respectively.

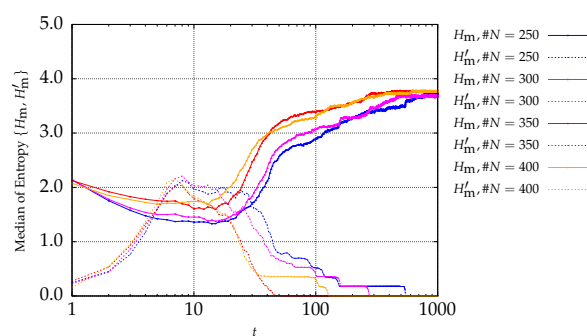


Figure 1. Evolution of H_m (continuous lines) and H'_m (dotted lines) versus the iterations t of the MSPSO iterations for P_1 and $\#A = 50$.

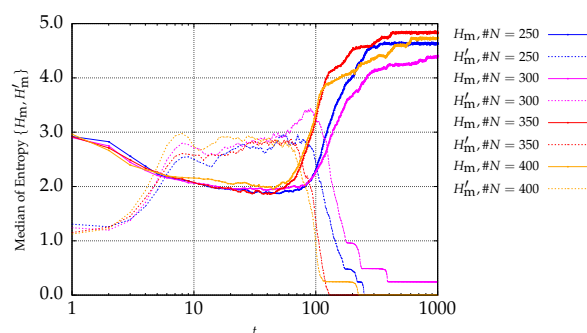


Figure 2. Evolution of H_m (continuous lines) and H'_m (dotted lines) versus the iterations t of the MSPSO iterations for P_1 and $\#A = 200$.

It can be observed that the two entropy signals are inversely correlated. In what concerns H'_m , it is verified that it starts with a low value and increases during the first iterations. Afterwards, H'_m remains almost stationary during some interactions and finally decreases to zero. This means that at the early stages, the number of fronts increases, remains constant during a certain number of iterations, and then decreases until only one front remains (i.e., the nondominated front), when

$H'_m = 0$. As the archive size increases, the initial transient takes more iterations, because as the number of archive size increases, it gets more difficult to find a larger number of nondominated particles in the same period. On the other hand, since the number of particles is larger, it is possible for more fronts to emerge. Therefore, H'_m takes more iterations to approach zero as the archive size increases.

Figures 3 and 4 present the entropy indices for the P_2 problem. A behavior similar to the one exhibited by P_1 is visible.

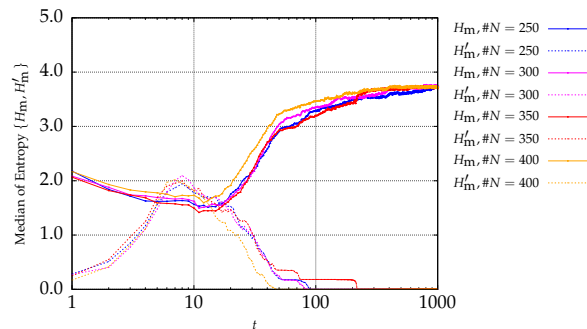


Figure 3. Evolution of H_m (continuous lines) and H'_m (dotted lines) versus the iterations t of the MSPSO iterations for P_2 and $\#A = 50$.

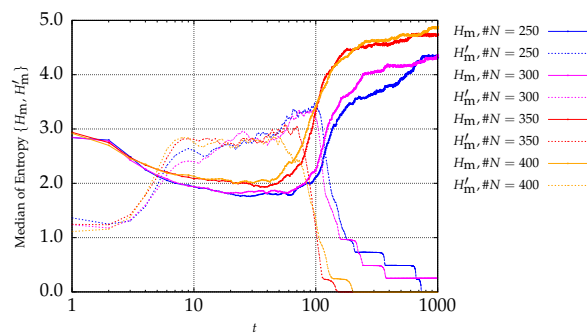


Figure 4. Evolution of H_m (continuous lines) and H'_m (dotted lines) versus the iterations t of the MSPSO iterations for P_2 and $\#A = 200$.

4.2. Results of P_3 Optimization

Figures 5 and 6 present the entropy indices for the P_3 problem. Here, H'_m starts by decreasing, showing that the number of fronts begins to reduce until only one front remains. Since the initial value of H'_m is low, the number of initial fronts is also small. On the other hand, the diversity between the particles begins with a high value and increases slightly during the iterations.

The number of fronts, i.e., the entropy front level diversity, can increase or decrease at early stages depending on the optimization problem.

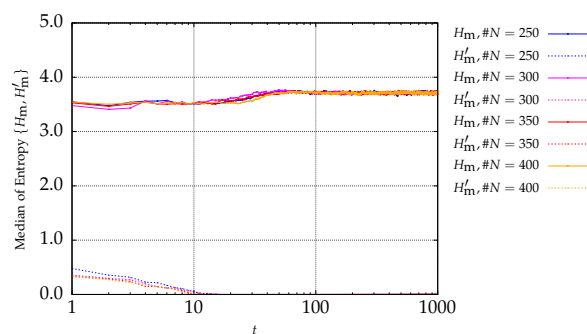


Figure 5. Evolution of H_m (continuous lines) and H'_m (dotted lines) versus the iterations t of the MSPSO iterations for P_3 and $\#A = 50$.

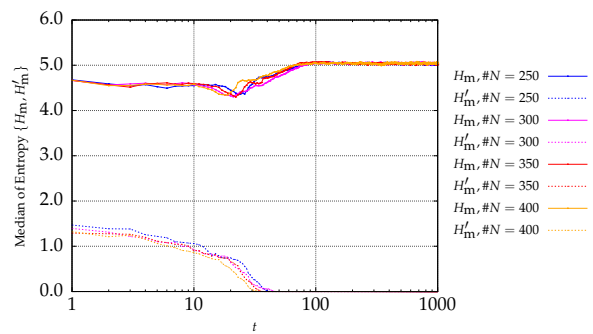


Figure 6. Evolution of H_m (continuous lines) and H'_m (dotted lines) versus the iterations t of the MSPSO iterations for P_3 and $\#A = 200$.

4.3. Correlation Coefficient

The results reveal a correlation between H_m and H'_m . The Pearson correlation coefficient r measures the strength and direction of a relationship between two indices, during $T = 10^3$ iterations:

$$r = \frac{\#A \sum_{t=1}^T H_m(t)H'_m(t) - \sum_{t=1}^T H_m(t) \sum_{t=1}^T H'_m(t)}{\sqrt{\left[\#A \sum_{t=1}^T H_m^2(t) - \left(\sum_{t=1}^T H_m(t) \right)^2 \right] \left[\#A \sum_{t=1}^T H'^2_m(t) - \left(\sum_{t=1}^T H'_m(t) \right)^2 \right]}}. \tag{11}$$

Table 1 presents the correlation between the particle diversity and front heterogeneity entropies. Column 1 indicates the archive size, column 2 stands for the swarm size, and the symbols r_1 , r_2 , and r_3 represent the correlation between H_m and H'_m for the problems P_1 , P_2 , and P_3 , respectively. An almost perfect negative relationship can be observed between them for each DTLZ problem. The relationship for the P_3 problem signals is moderate for the archive size of $\#A = 50$ particles, but it is stronger for the other archive sizes. These values of r demonstrate that the 2 indices are in good agreement, concluding that the diversity solution is highly correlated in the number of fronts.

Table 1. Pearson correlation coefficient r between H_m and H'_m .

Archive Size (A_p)	Swarm Size (N_p)	r_1	r_2	r_3
50	250	-0.97	-0.92	-0.51
	300	-0.97	-0.92	-0.66
	350	-0.88	-0.96	-0.50
	400	-0.93	-0.89	-0.43
100	250	-0.99	-0.99	-0.81
	300	-0.99	-0.92	-0.69
	350	-0.97	-0.96	-0.73
	400	-0.96	-0.95	-0.75
150	250	-0.98	-0.98	-0.82
	300	-0.98	-0.99	-0.74
	350	-0.97	-0.99	-0.80
	400	-0.98	-0.97	-0.69
200	250	-0.99	-0.98	-0.81
	300	-0.98	-0.98	-0.72
	350	-0.97	-0.98	-0.75
	400	-0.96	-0.98	-0.77

4.4. Archive Evolution

In order to show the particle distribution of the archive, the position of the particles archive is plotted at $t = \{0, 3, 80, 110, 400, 1000\}$ iterations, for problem P_2 , with $\#N = 250$ and $\#A = 200$. The iterations are chosen at different stages of the evolution, namely, at the beginning ($t = 1$), when the diversity index drops down ($t = 4$), at the end of this stagnation phase ($t = 80$), after an abrupt increase of the index ($t = 110$), after some iterations ($t = 400$), and at the end of the run ($t = 1000$). The plots represented in Figure 7 illustrate the result for one single run.

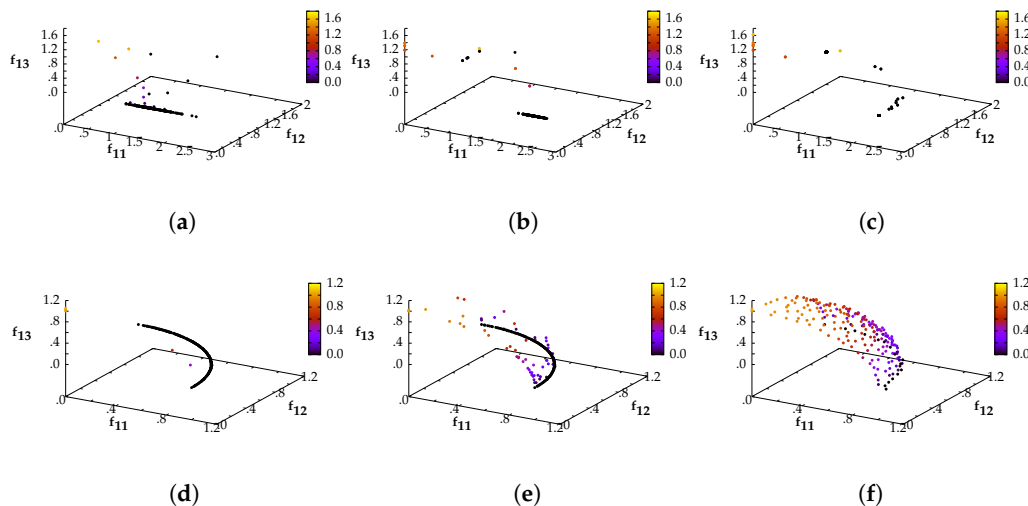


Figure 7. MPO evolution for an isolated run of the P_2 problem with $\#N = 250$ and $\#A = 200$ for iteration (a) $t = 1$, (b) $t = 4$, (c) $t = 80$, (d) $t = 110$, (e) $t = 400$ and (f) $t = 1000$.

It can be observed that the entropy achieves the maximum value when the archive solutions are well dispersed.

5. Conclusions and Future Work

Two indices based on entropy were proposed to characterize the MOPSO dynamics. This work measures the diversity of the archive during the evolution, adopting one possible interpretation of entropy. The first index, the particle diversity, is used to measure the archive diversity between particles. The second index, borrowed from ecology, measures the species heterogeneity, in this case the front level heterogeneity. The indices were evaluated using different approaches, but both entropy indices were in good agreement, revealing that solution diversity is correlated with the number of fronts. The particle diversity indices when stagnated reveal that the algorithm has converged. On the other hand, the front level heterogeneity, when reaching zero, indicates that there is only one front in the archive.

For most MOPSO reported in the literature, the performance evaluation is analyzed at the end of the algorithm, by comparing the final front extension, spreading, and diversity. The indices formulated in this paper can be used to analyze the convergence rate during the time evolution. In future work, the indices will be used to identify stagnated stages of MOPSO and introduce mechanisms to promote the dispersion of particles during evolution optimization.

Author Contributions: All authors contributed equally to the paper.

Funding: This research received no external funding.

Conflicts of Interest: The authors declare no conflicts of interest.

References

1. Qu, B.; Zhu, Y.; Jiao, Y.; Wu, M.; Suganthan, P.; Liang, J. A survey on multi-objective evolutionary algorithms for the solution of the environmental/economic dispatch problems. *Swarm Evol. Comput.* **2018**, *38*, 1–11. [[CrossRef](#)]
2. Kennedy, J. Particle swarm optimization. In Proceedings of the 1995 IEEE International Conference on Neural Networks, Perth, Australia, 27 November–1 December 1995; Volume 4, pp. 1942–1948.
3. Goldberg, D.E. *Genetic Algorithms in Search, Optimization, and Machine Learning*; Addison–Wesley: Boston, MA, USA, 1989.
4. Deb, K. *Multi-Objective Optimization using Evolutionary Algorithms*; John Wiley & Sons: Hoboken, NJ, USA, 2001.
5. Coello, C.A.C.; Lechuga, M. MOPSO: A proposal for multiple objective particle swarm optimization. In Proceedings of the 2002 Congress on Evolutionary Computation, CEC'02 (Cat. No.02TH8600), Honolulu, HI, USA, 12–17 May 2002; Volume 2, pp. 1051–1056. [[CrossRef](#)]
6. Reyes-Sierra, M.; Coello, C. Multi-objective particle swarm optimizers: A survey of the state-of-the-art. *Int. J. Comput. Intell. Res.* **2006**, *2*, 287–308.
7. Zhou, A.; Qu, B.Y.; Li, H.; Zhao, S.Z.; Suganthan, P.N.; Zhang, Q. Multiobjective evolutionary algorithms: A survey of the state of the art. *Swarm Evol. Comput.* **2011**, *1*, 32–49. [[CrossRef](#)]
8. Zhao, S.Z.; Suganthan, P.N. Two-lbests based multi-objective particle swarm optimizer. *Eng. Optim.* **2011**, *43*, 1–17. [[CrossRef](#)]
9. Freire, H.; Moura Oliveira, P.B.; Solteiro Pires, E.J. From single to many-objective PID controller design using particle swarm optimization. *Int. J. Control Autom. Syst.* **2017**, *15*, 918–932. [[CrossRef](#)]
10. Riquelme, N.; Lücken, C.V.; Baran, B. Performance metrics in multi-objective optimization. In Proceedings of the 2015 Latin American Computing Conference (CLEI), Arequipa, Peru, 19–23 October 2015; pp. 1–11. [[CrossRef](#)]
11. Derrac, J.; García, S.; Molina, D.; Herrera, F. A practical tutorial on the use of nonparametric statistical tests as a methodology for comparing evolutionary and swarm intelligence algorithms. *Swarm Evol. Comput.* **2011**, *1*, 3–18. [[CrossRef](#)]
12. Solteiro Pires, E.J.; de Moura Oliveira, P.B.; Tenreiro Machado, J.A. Multi-objective MaxiMin Sorting Scheme. In Proceedings of the Conference on Evolutionary Multi-criterion Optimization—EMO 2005, Guanajuato, Mexico, 9–11 March 2005; Lecture Notes in Computer Science Volume 3410; Springer: Guanajuato, Mexico, 2005; pp. 165–175.
13. Wang, L.; Chen, Y.; Tang, Y.; Sun, F. The entropy metric in diversity of Multiobjective Evolutionary Algorithms. In Proceedings of the 2011 International Conference of Soft Computing and Pattern Recognition (SoCPaR), Dalian, China, 14–16 October 2011; pp. 217–221. [[CrossRef](#)]
14. LinLin, W.; Yunfang, C. Diversity Based on Entropy: A Novel Evaluation Criterion in Multi-objective Optimization Algorithm. *Int. J. Intell. Syst. Appl.* **2012**, *4*, 113–124.
15. Farhang-Mehr, A.; Azarm, S. Diversity assessment of Pareto optimal solution sets: An entropy approach. In Proceedings of the 2002 Congress on Evolutionary Computation (CEC'02), Honolulu, HI, USA, 12–17 May 2002; Volume 1, pp. 723–728. [[CrossRef](#)]
16. Deb, K.; Jain, S. *Running Performance Metrics for Evolutionary Multi-Objective Optimization*; Technical Report 2002004; Indian Institute of Technology: Kanpur, India, 2002.
17. Myers, R.; Hancock, E.R. Genetic algorithms for ambiguous labelling problems. *Pattern Recognit.* **2000**, *33*, 685–704. [[CrossRef](#)]
18. Solteiro Pires, E.J.; Tenreiro Machado, J.A.; de Moura Oliveira, P.B. Dynamical Modelling of a Genetic Algorithm. *Signal Process.* **2006**, *86*, 2760–2770. [[CrossRef](#)]
19. Solteiro Pires, E.J.; Tenreiro Machado, J.A.; de Moura Oliveira, P.B. Entropy Diversity in Multi-Objective Particle Swarm Optimization. *Entropy* **2013**, *15*, 5475–5491. [[CrossRef](#)]
20. Solteiro Pires, E.J.; Tenreiro Machado, J.A.; de Moura Oliveira, P.B. Diversity study of multi-objective genetic algorithm based on Shannon entropy. In Proceedings of the 2014 Sixth World Congress on Nature and Biologically Inspired Computing (NaBIC 2014), Porto, Portugal, 30 July–1 August 2014; pp. 17–22. [[CrossRef](#)]
21. Wu, C.; Wu, T.; Fu, K.; Zhu, Y.; Li, Y.; He, W.; Tang, S. AMOBH: Adaptive Multiobjective Black Hole Algorithm. *Comput. Intell. Neurosci.* **2017**, *2017*, 6153951. [[CrossRef](#)] [[PubMed](#)]

22. Seneta, E. A Tricentenary history of the Law of Large Numbers. *Bernoulli* **2013**, *19*, 1088–1121. [[CrossRef](#)]
23. Ben-Naim, A. *Entropy and the Second Law: Interpretation and Miss-Interpretations*; World Scientific Publishing Company: Singapore, 2012.
24. Shannon, C.E. A Mathematical Theory of Communication. *Bell Syst. Tech. J.* **1948**, *27*, 379–423, 623–656. [[CrossRef](#)]
25. Solteiro Pires, E.J.; Tenreiro Machado, J.A.; de Moura Oliveira, P.B. Multi-objective Dynamic Analysis Using Fractional Entropy. In *Intelligent Systems Design and Applications*; Madureira, A.M., Abraham, A., Gamboa, D., Novais, P., Eds.; Springer International Publishing: Cham, Switzerland, 2017; pp. 448–456.
26. Pielou, E.C. Shannon's Formula as a Measure of Specific Diversity: Its Use and Misuse. *Am. Nat.* **1966**, *100*, 463–465. [[CrossRef](#)]
27. Morris, E.K.; Caruso, T.; Buscot, F.; Fischer, M.; Hancock, C.; Maier, T.S.; Meiners, T.; Maller, C.; Obermaier, E.; Prati, D.; et al. Choosing and using diversity indices: Insights for ecological applications from the German Biodiversity Exploratories. *Ecol. Evol.* **2018**, *18*, 3514–3524. [[CrossRef](#)] [[PubMed](#)]
28. Shannon, C.E.; Weaver, W. *The Mathematical Theory of Communication*; University of Illinois Press: Champaign, IL, USA, 1963.
29. Deb, K.; Thiele, L.; Laumanns, M.; Zitzler, E. Scalable Multi-Objective Optimization Test Problems. In Proceedings of the 2002 Congress on Evolutionary Computation, CEC'02 (Cat. No.02TH8600), Honolulu, HI, USA, 12–17 May 2002.
30. Zhang, Q.; Zhou, A.; Zhao, S.; Suganthan, P.N.; Liu, W.; Tiwari, S. *Multiobjective Optimization Test Instances for the CEC 2009 Special Session and Competition*; Technical Report CES-487; University of Essex and Nanyang Technological University: Essex, UK, 2008.



© 2019 by the authors. Licensee MDPI, Basel, Switzerland. This article is an open access article distributed under the terms and conditions of the Creative Commons Attribution (CC BY) license (<http://creativecommons.org/licenses/by/4.0/>).